Soft Matter

PAPER

View Article Online
View Journal | View Issue

Cite this: *Soft Matter*, 2015, **11**, 2085

Celebrating Soft Matter's 10th Anniversary: Chain configuration and rate-dependent mechanical properties in transient networks†

Michelle K. Sing,[a] Zhen-Gang Wang,[b] Gareth H. McKinley*[c] and Bradley D. Olsen*[d]

Received 30th September 2014
Accepted 3rd December 2014

DOI: 10.1039/c4sm02181a

www.rsc.org/softmatter

Numerical solution of a coupled set of Smoluchowski convection-diffusion equations of associating polymers modelled as finitely extensible dumbbells enables computation of time-dependent end-to-end distributions for bridged, dangling, and looped chains in three dimensions as a function of associating end-group kinetics. Non-monotonic flow curves which can lead to flow instabilities during shear flow result at low equilibrium constant and high association rate from two complementary phenomena: a decrease in the fraction of elastically active chains with increasing shear rate and non-monotonic extension in the population of elastically active chains. Chain tumbling leads to reformation of bridges, resulting in an increased fraction of bridged chains at high Deborah number and significant reduction in the average bridge chain extension. In the start-up of steady shear, force-activated chain dissociation and chain tumbling cause both stress overshoot and stress ringing behaviour prior to reaching steady state stress values. During stress relaxation following steady shear, chain kinetics and extension mediate both the number of relaxations and the length of time required for system relaxation. While at low association rate relaxation is limited by the relaxation of dangling chains and the rate of dangling chain formation, at high association rate coupling of dangling and bridged chains leads to simultaneous relaxation of all chains due to a dynamic equilibrium between dangling and bridged states.

Introduction

Polymer gels have attracted a great deal of attention as soft electronics and sensors,[1–3] decontamination devices,[4,5] tissue engineering scaffolds,[3,6,7] and drug delivery carriers.[3,6,7] In each of these applications, control over gel structure and mechanics is critical to obtaining the desired gel behaviour.[8] Many such materials incorporate transient networks, where the use of physical associations as opposed to permanent chemical bonds allows the gels to respond to environmental stimuli such as temperature,[9] pH,[10] ionic strength,[11] and light.[12] These types of physically associated networks also demonstrate mechanical properties not seen in their chemically crosslinked counterparts, including shear thinning at high strain rates, self-healing properties, and stress relaxation at long times. This combination of responsive and mechanical properties makes physically associated networks ideally suited for a wide variety of applications in natural and synthetic materials: mussel byssus,[13] mucus,[10] shear-thinning injectable gels,[14,15] sensors,[1] drug delivery vessels,[16–18] and tissue replacement.[18,19] Because the mechanical properties of these materials are critical to their use in natural or engineered applications, a fundamental understanding of physically associating network dynamics is critical to the design of these systems and to understanding nature's solutions to engineering problems.

Transient network theory provides a framework for modelling the rheology of associating polymers using coarse-grained molecular properties such as association energies, degrees of polymerization, and associating group molecular geometries. Transient network theory has its roots in rubber elasticity theory, which connects the internal stress of a polymer to its change in entropy.[20,21] In the original transient network theory, Green and Tobolsky attributed the stress relaxation seen in rubbers to the relaxation of physical entanglements.[22] Tanaka and Edwards expanded the ideas of Green and Tobolsky to a physically associating network.[23] When a chain is pulled out of a junction, the chain has a finite time on the order of its relaxation time after which it no longer remembers the stress.[23] These ideas have been applied to multiple other systems in order to take into account the effects of network topology,[24] multifunctional stickers,[25] non-telechelic associations,[26] and the presence of intrachain associations[27] on the free energy of a system.

[a]*Department of Materials Science and Engineering, Massachusetts Institute of Technology, Cambridge, MA 02139, USA*

[b]*Department of Chemical Engineering, California Institute of Technology, Pasadena, CA 91125, USA*

[c]*Department of Mechanical Engineering, Massachusetts Institute of Technology, Cambridge, MA 02139, USA. E-mail: gareth@mit.edu*

[d]*Department of Chemical Engineering, Massachusetts Institute of Technology, Cambridge, MA 02139, USA. E-mail: bdolsen@mit.edu*

† Electronic supplementary information (ESI) available. See DOI: 10.1039/c4sm02181a

All of the aforementioned theories utilize system thermodynamics to determine gel mechanical properties. While other approaches take into account location-dependent chain end associations using Brownian dynamics[28,29] simulations, many experimental reports have implicitly or explicitly shown the importance of sticker dynamics on viscoelastic properties.[14,30–34] Tripathi *et al.* address this by combining kinetic theory calculations with the conformational and chain elasticity dependence from Tanaka and Edwards, Annable, Semenov and others.[35] The rates of association and dissociation of chains from their network junctions are affected by the surrounding energy landscape. Instead of treating only bridging chains as active, Tripathi *et al.* also included dangling chains when calculating the resultant mechanical behaviour.[35] More recently, Frederickson and Hoy addressed the chemical kinetic contribution to the behaviour of associating polymer networks *via* chemical reaction equilibrium, assuming an Arrhenius two-state model where sticky bonds are either bound or unbound.[36] Both of these papers, amongst others that address either kinetic limitation *via* diffusion[36,37] or dependence upon the system dynamics,[36–40] still neglect the effect of looped chains on the resultant mechanical properties and do not track the entire chain conformational distribution. Both of these aspects were shown to be important in the context of previous theories – Annable *et al.*'s thermodynamic treatment of network topology to include characteristics like loops and superloops in the macroscopic stress behaviour,[24] and Cifre *et al.*'s Brownian dynamics simulations to include location dependence on association kinetics in order to better capture strain thickening behaviour.[28]

This work presents a modified transient network theory capable of calculating associated polymer rheological properties under time-dependent shear. The numerical solution of a coupled set of Smoluchowski equations is used to quantitatively model the chain end probability distribution of bridged, dangling, and looped chains. From this theory, a connection between the system kinetics for association and dissociation, the rate of association relative to chain relaxation on one hand, and the stability of the macroscopic stress response on the other, becomes apparent. The impact of both loop formation and chain tumbling on mechanical response in telechelic polymer gels is explored for the first time.

Theory and numerical methodology

Bead-spring chain model

The transient networks modelled here are composed of telechelic polymers capable of forming a network of associated domains in solution (Fig. 1a). Assuming that chains in the network behave independently, polymers obey Rouse dynamics, and the flow is homogeneous, the distribution of chain configurations within the network as a function of time may be modelled by solving the Smoluchowski equation for the probability density of a single chain of length N. Deformation processes are modelled in the frame of reference of one of the chain ends, effectively restricting one chain end to the origin. This assumption results in no loss in generality, as the chain

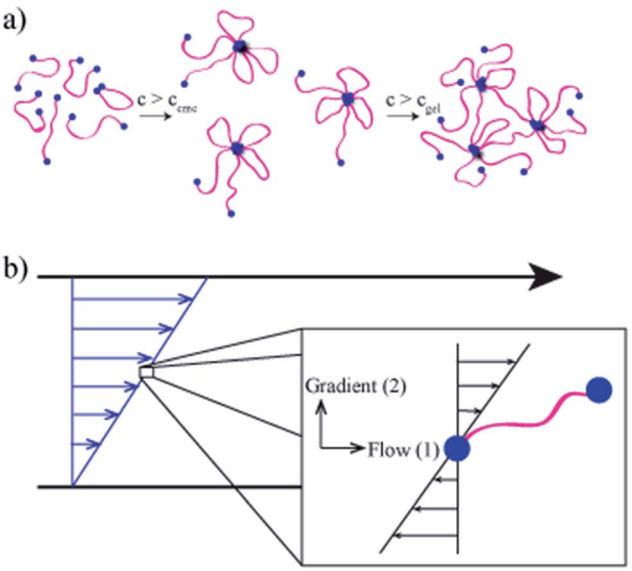

Fig. 1 (a) Schematic of telechelic polymer gelation showing formation of micelles above the critical micelle concentration followed by the formation of a physically associating polymer network above the gel concentration. (b) Flow schematic of a single chain in macro and microscopically homogeneous shear flow. Calculations are performed in the reference frame of one chain end.

end distribution and all equations have inversion symmetry such that the ends may be exchanged without any impact on the physics of the problem. The second chain end is allowed to react with the surrounding network, transitioning between dangling, bridged, and looped states as a function of its conformation and chain end kinetics. The relevant equations are based on the Smoluchowski equation for convection, reaction, and diffusion.[41–43]

$$\frac{\mathrm{d}\psi_i(r,t)}{\mathrm{d}t} = \vec{\nabla}\cdot\left[2D_{tr}\vec{\nabla}\psi_i + \frac{2\psi_i}{\zeta}\vec{\nabla}U\right] + \vec{\nabla}\cdot\vec{v}\psi_i + R_{ij} \quad (1)$$

here, $\psi_i(r,t)$ is the chain density probability distribution function for species i (i = D, L, B for dangling, looped and bridged), D_{tr} is the diffusion coefficient, ζ is the friction factor, $\vec{\nabla}U$ is the retraction force due to chain stretching, $\vec{v}$ is the external fluid velocity, and R_{ij} is the reaction rate for conversion from species i to species j. Each type of chain connectivity (bridged, looped, dangling) is represented by a separate Smoluchowski equation, with coupling between the three equations through the reaction terms.

Four reactions are allowed to occur *via* the reversible conversion of dangling chains to loops and bridges. The rate constants for association and dissociation reactions are assumed to be identical regardless of whether a loop or bridge is being formed or broken. Whether a dangling chain end associates to form a loop or a bridge is determined based on the end-to-end distance of the polymer chain, where the conditional probability of forming a loop given that a chain end has associated with the network is assumed to follow a Gaussian probability distribution

$$f(\tilde{r}) = \exp(-\tilde{r}^2/\chi) \quad (2)$$

where $f(\tilde{r}=0)=1$ and $\tilde{r}$ represents a dimensionless distance as defined below. For purposes of this work, the Gaussian width χ is set to $0.25Nb^2$. The value for χ comes from Brownian dynamics, where the range of interaction between two chain ends for associative networks is $\chi=(0.5\sqrt{Nb^2})^2=0.25Nb^2$.[29]

The rate of reaction for endgroup dissociation from bridges is determined using Bell's law for specific adhesion, where the work required to break a bond is exponentially related to the retraction force acting on the length of the bond.[44–46]

$$R_{\text{Bridge dissociation}}=k_{\text{d}}\exp(\tilde{\beta}|\tilde{F}_{\text{FENE}}|) \tag{3}$$

here, $\tilde{\beta}$ corresponds to the dimensionless characteristic bond length, which for purposes of this work was set to 0.35 in units of R_{g}, approximately corresponding to a larger associating domain such as a polymer endblock,[47] protein coiled-coil,[48,49] or long chain alkyl hydrophobe,[50] all of which form aggregates with a characteristic dimension of 2–40 nm. The force $\tilde{F}$ corresponds to the dimensionless spring retraction force.[44–46] The spring retraction is represented using the finitely extensible non-linear elastic (FENE) force law:

$$F_{\text{FENE}}=\frac{3k_{\text{B}}T}{Nb^2}\frac{r}{1-(r/L)^2} \tag{4}$$

The coefficient $3k_{\text{B}}T/Nb^2$ in eqn (4) is the Hookean spring constant for a Gaussian chain in 3-D and $\text{L}=Nb$ corresponds to the contour length of a polymer chain of N segments, each of size b.

The final form of all three evolution equations can then be determined, assuming that the chain end of a looped chain does not experience convection or diffusion and the chain end of a bridged chain is deformed affinely with the flow field. Defining the equilibrium constant $K_{\text{eq}}=\tilde{k}_{\text{d}}/\tilde{k}_{\text{a}}$, and non-dimensionalizing the equations by the variables,

$$\begin{aligned} t&=\tau\tilde{t}\\ r&=\sqrt{Nb^2}\tilde{r},\\ \vec{\nabla}&=\frac{\tilde{\nabla}}{\sqrt{Nb^2}} \end{aligned} \tag{5}$$

where τ represents the relaxation time for a single dumbbell, yields the final equations:

$$\begin{aligned} \frac{\text{d}\psi_{\text{D}}}{\text{d}\tilde{t}}&=(1/3)\tilde{\nabla}_{\text{r}}{}^2\psi_{\text{D}}+\tilde{\nabla}_{\text{r}}\cdot\left(\psi_{\text{D}}\tilde{F}_{\text{FENE}}\right)\\ &-\text{De}\cdot\tilde{r}_{\text{y}}\tilde{\nabla}_{\text{r}}\psi_{\text{D}}-(1-f(\tilde{r}))\tilde{k}_{\text{a}}\psi_{\text{D}}+\tilde{k}_{\text{a}}K_{\text{eq}}\psi_{\text{B}}\text{e}^{\tilde{\beta}|\tilde{F}_{\text{FENE}}|}\\ &-f(\tilde{r})\tilde{k}_{\text{a}}\psi_{\text{D}}+\frac{f(\tilde{r})}{\int f(\tilde{r})\text{d}\tilde{r}}\tilde{k}_{\text{a}}K_{\text{eq}}\psi_{\text{L}} \end{aligned} \tag{6}$$

$$\frac{\text{d}\psi_{\text{B}}}{\text{d}\tilde{t}}=\text{De}\cdot\tilde{r}_{\text{y}}\tilde{\nabla}_{\text{r}}\psi_{\text{B}}+\left(1-f\left(\tilde{r}\right)\right)\tilde{k}_{\text{a}}\psi_{\text{D}}-\tilde{k}_{\text{a}}K_{\text{eq}}\psi_{\text{B}}\text{e}^{\tilde{\beta}|\tilde{F}_{\text{FENE}}|} \tag{7}$$

$$\frac{\text{d}\psi_{\text{L}}}{\text{d}\tilde{t}}=\tilde{k}_{\text{a}}\int f\left(\tilde{r}\right)\psi_{\text{D}}\text{d}\tilde{r}-\tilde{k}_{\text{a}}K_{\text{eq}}\psi_{\text{L}} \tag{8}$$

The first three terms in eqn (6) correspond to chain end diffusion, retraction, and convection (respectively). The subsequent two terms correspond to the creation and destruction of bridged chains from dangling chains, and the last two to the creation and destruction of looped chains from dangling chains. Eqn (7) and (8) contain similar terms as a function of expected chain end behaviour. The Deborah number (De) and $\tilde{k}_{\text{a}}$ correspond to the dimensionless shear rate and dimensionless association rate, respectively, non-dimensionalized by the chain relaxation time, τ. For simplicity, hydrodynamic interactions are neglected. While it is expected that this will not impact the qualitative nature of the results, the assumption of a freely draining network will impact the quantitative values of the stress response.

Numerical solution of the Smoluchowski equation

In order to solve the system of eqn (6)–(8), *Matlab* was used to implement a modified fourth-order Runge–Kutta (RK4) algorithm adapted from Recktenwald.[51] Equations were re-written in their discretized form in a 3-D mesh. The diffusive terms are represented using a second order central difference equation and the convective terms are represented using a combination of second order forward and backward differences. These particular difference formulas were chosen in order to maximize stability while minimizing computational time. Each run was pre-equilibrated from the initial condition of a free Gaussian chain following the equation

$$\psi_{\text{D}}(\tilde{r},0)=\frac{3}{2\pi}\exp\left(\frac{-3\tilde{r}^2}{2}\right) \tag{9}$$

by letting the system run without flow to allow for the looped, bridged, and free chains to equilibrate with one another (ESI†).

The stress was determined from the configurational average of the product of the imposed retraction force in direction 1 and the distance in direction 2. Taking into account both the bridged and dangling chains (Fig. 1b),

$$\tilde{\sigma}_{12}=\frac{\sigma_{12}}{\nu k_{\text{B}}T}=3\sum_i\sum_j\sum_k\left[\left(\psi_{\text{D}_{i,j,k}}+\psi_{\text{B}_{i,j,k}}\right)\tilde{F}_{1_{i,j,k}}\tilde{r}_{2_{i,j,k}}\right] \tag{10}$$

For purposes of this work, subscripts 1 and 2 in eqn (10) represent the flow and gradient directions, respectively.

The equations were numerically solved in three dimensions under imposed step shear profiles, allowing both steady shear and start-up shear to be analysed. Details regarding convergence to steady state, determination of time step size for stability, and the mesh size used can be found in the ESI.†

Results and discussion

Effect of reaction kinetics on non-monotonic stress behaviour in steady shear

The endgroup association equilibrium constant and rate constant are the primary determinants of flow stability in telechelic gels. The kinetic interchange between bridged and

dangling chains is well known to lead to non-monotonic flow curves in telechelic gels due to a decrease in the average chain extension with increasing shear.[41] Non-monotonic flow curves occur when the stress decreases with increasing shear rate.[52] This occurs because bridged chains deform affinely with the network while dangling chains are increasingly stretched with increasing strain rates. Shifting of the equilibrium between bridged and dangling chains at high shear rate can therefore lead to a decrease in chain extension and consequently in the total stress, with increasing shear rate. To quantify this effect in our model, the development of non-monotonic flow curves was systematically investigated as a function of $\tilde{k}_a$ and K_{eq}. Experimentally, K_{eq} can be controlled through the binding interaction of the associating groups according to the Van't Hoff equation, and since $K_{eq} = \tilde{k}_d/\tilde{k}_a$ either rate constant can be controlled independently to set the dynamics of bond exchange in the system. A value of $\tilde{k}_a$ less than unity corresponds to a chain with an association rate that is slower than the chain's relaxation rate $1/\tau$ where τ is:

$$\tau = \frac{\zeta N b^2}{6 k_B T} \tag{11}$$

Lower values of K_{eq} represent cases where association is faster than dissociation.

Both decreasing $\tilde{k}_a$ and decreasing K_{eq} promote the development of non-monotonic flow curves (Fig. 2a and b). Non-monotonic flow profiles, indicated by dashed lines in Fig. 2a, occur when the stress as a function of De has a negative slope.[53,54] Specifically, any system where the first derivative of the stress, d(log $\tilde{\sigma}$)/d(log De), is negative becomes unstable. A map of the stress behaviour as a function of system kinetics (Fig. 2b) indicates that at low values of $\tilde{k}_a$ and K_{eq}, the system has regions of non-monotonicity (detailed data shown in Fig. S4†). However, when the values of $\tilde{k}_a$ and K_{eq} are increased, the system transitions to a flow curve with monotonically-increasing stress as a function of shear rate.

Familiar limiting regimes can be identified on this graph: for high K_{eq} and any value of $\tilde{k}_a$, the material becomes a non-associating polymer fluid, following the Maxwell model in this simulation. As $\tilde{k}_a$ is decreased, making crosslinks effectively more permanent, the value of K_{eq} required to reach this regime increases. The chemically crosslinked gel regime is associated with low K_{eq} and low $\tilde{k}_a$, where non-monotonic stress profiles are consistent with chain extension and breaking to form dangling chains in the chemical gels.

Replotting the data from Fig. 2 to be a log–log representation of $\tilde{k}_a$ and $\tilde{k}_d$ results in a transition line around a constant value $\tilde{k}_d = 0.01$, suggesting a critical value of $\tilde{k}_d$ for the onset of non-monotonic stress behaviour over the range of the simulations. However, analysis of limiting regimes indicates that this critical value is observed over a limited range of parameter space. In the limiting case where $\tilde{k}_a$ is much higher than $\tilde{k}_d$ (small K_{eq}) and much larger than unity the stress will increase monotonically due to the coupled extension of dangling and bridged chains. At low chain extension, the dominant bridge population will deform affinely with the network; however, at large extension

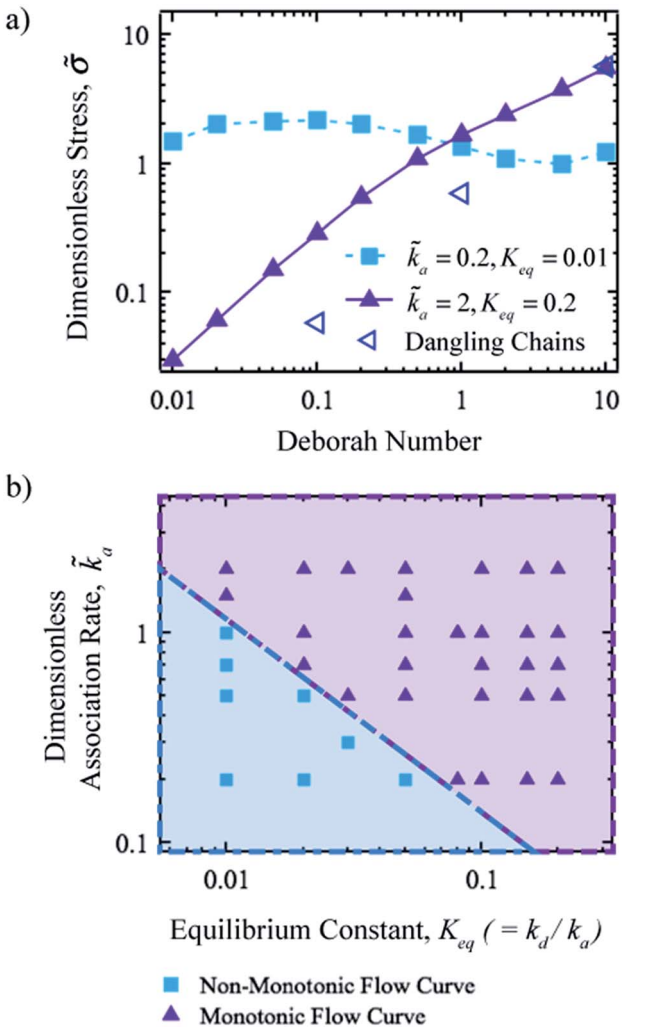

Fig. 2 (a) Transient network behaviour under steady shear for two different systems, one undergoing stress non-monotonicities ($\tilde{k}_a$ = 0.2, K_{eq} = 0.01) and the other with monotonically increasing stress ($\tilde{k}_a$ = 2, K_{eq} = 0.2). The dangling chain stress is shown for De = 0.1, 1, and 10 in order to illustrate the role of dangling chains. (b) Phase map indicating regions of stress behaviour corresponding to two types of curves in (a). Stress non-monotonicities in the lower left region are to be expected due to non-monotonic behaviour, while monotonic behaviour occurs in the upper right region.

force-activated dissociation will balance rapid association. Under these conditions, rapid interchange of the dangling and bridged chain populations results in coupled extension of dangling and bridged chains, yielding monotonic extension of a single chain population that is in rapid dynamic equilibrium between dangling and bridged populations. This suggests that at low K_{eq} there will be an upper limit of $\tilde{k}_a$ above which non-montonic flow curves cannot form, with lower K_{eq} yielding higher extension required to balance association and dissociation for a given $\tilde{k}_a$.

Similarly, when the material behaves as a non-associating polymer fluid ($\tilde{k}_a \ll \tilde{k}_d$) and $\tilde{k}_a$ is very small, the stress is also expected to increase monotonically with increasing shear rate because partially extended dangling chains dominate the

polymeric stress. This suggests an upper limit of K_{eq} above which stress these stress non-monotonicities cannot occur. Therefore, in both low and high K_{eq} limits, the critical value of $\tilde{k}_d$ is not expected to be observed.

Because the stress in the network is a function of chain extension and the number of elastically contributing chains (bridges and dangling chains; eqn (10)), non-monotonic stress profiles may result from either changes in the average chain extension of bridges and dangling chains or from changes in the populations of looped, bridged, and dangling chains. Since the deformation of both bridged and dangling chains in isolation increases with increasing shear rate, a decrease in average chain extension must stem from the dynamic interchange between bridges, loops, and dangling chains as part of the flow process.

Calculations show that changes in both the number of looped chains and in the average extension of dangling and bridged chains contribute to the development of non-monotonic flow curves. Fig. 3 shows the number of elastically active chains, the stress per elastically active chain, and the total stress as a function of De for a variety of different values of K_{eq} and $\tilde{k}_a$. It is clear that non-monotonicities exist in the stress per elastically active chain due to non-monotonic changes in dangling and bridged chain extension (Fig. 3a, d and g). However, the onset of these non-monotonicities in the total stress curve is shifted to lower stress by decreases in the number of elastically active chains at intermediate values of De for many systems. Therefore, both looping and chain extension play a critical role in non-monotonic stresses.

When computations are performed without any looped chains, the stress per elastically active chain is identical to that obtained in the presence of loops (ESI†). The presence of loops only serves as a way to decrease the number of elastically effective chains present in the system. This overlap between the

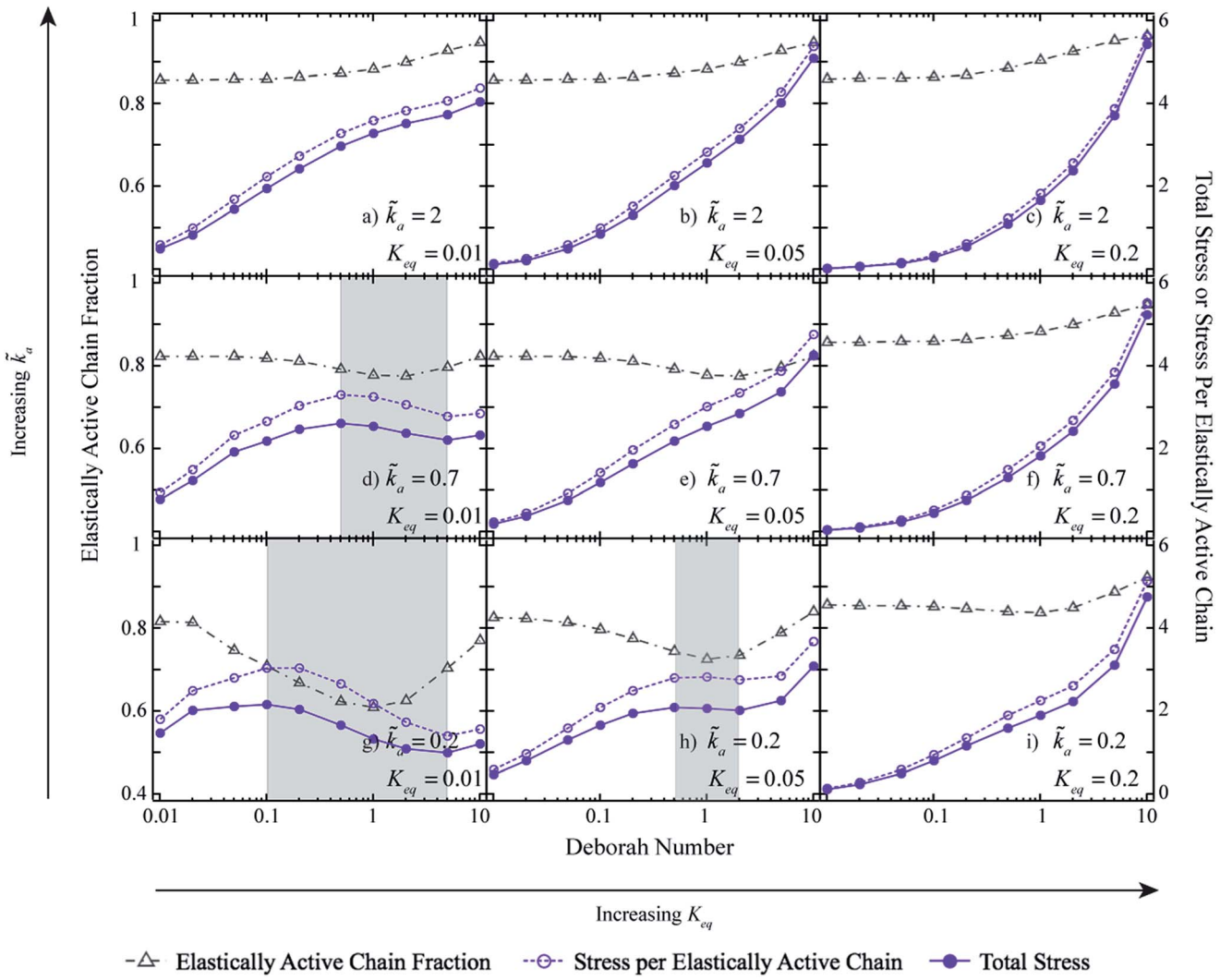

Fig. 3 Comparison of the stress per elastically active chain, the total stress, and the fraction of elastically-active chains. Grey regions indicate regions with non-monotonic steady state stress behaviour. Non-monotonicities in the stress per elastically active chain occur in tandem with the corresponding stress non-monotonicities. The total fraction of elastically active chains decreases with decreasing K_{eq}, and non-monotonicities develop with decreasing $\tilde{k}_a$. The stress per elastically active chain is the same as the stress of a system that does not incorporate the ability to form looped chains over the range of parameters explored.

stress per elastically active chains and the total stress for a system where loops cannot form indicates that the effects of looping and chain extension may be considered separately over this range of simulation parameters. Therefore, careful examination of both the chain fraction and polymer extension as a function of the reaction kinetics during deformation is critical to understanding the molecular mechanisms underlying these effects.

Effect of relative loop and bridge fractions on steady shear mechanical response

Traditional transient network theory assumes a decrease in association fraction with increasing shear rate.[23] When K_{eq} and $\tilde{k}_a$ are larger, such behaviour is observed in the model presented here (Fig. 4b). As De increases, the overall fraction of associated chains (bridged and looped) decreases from the expected equilibrium value. The decrease in bridged chain fraction is caused by force-activated dissociation at high chain extension, while the decrease in looped chain fraction is caused by the dynamic equilibrium between dangling chains and loops. As the average extension of dangling chains increases, they become less likely to react to form loops and more likely to form bridges. When loops break, the dangling chains become extended in a strong shear flow and are unlikely to reform loops. Therefore, both looped and bridged chain associations decrease with increasing Deborah number for De > 1 where the convective forces cause significant distortion of dangling chains from their equilibrium configuration.

However, as K_{eq} or $\tilde{k}_a$ is decreased, the behaviour of the system changes. For low De, the fraction of bridged chains still decreases with increasing De, resulting in a monotonic increase in the density of dangling chains for all $\tilde{k}_a$ and K_{eq}. However, the density of looped chains may increase or decrease relative to the zero shear value depending upon the magnitude of the reaction rate. The increased rate of interconversion between bridged and dangling chains at high $\tilde{k}_a$ results in higher dangling chain extension, which disfavours loop formation and therefore results in a decrease in loops at low shear. In contrast, when the rate of association $\tilde{k}_a$ is low (*i.e.* $k_a < \tau^{-1}$), dangling chains are able to relax prior to re-association and are more likely to form loops. The loop fraction can then exceed the equilibrium value because the increased concentration of dangling chains promotes loop formation at an enhanced rate.

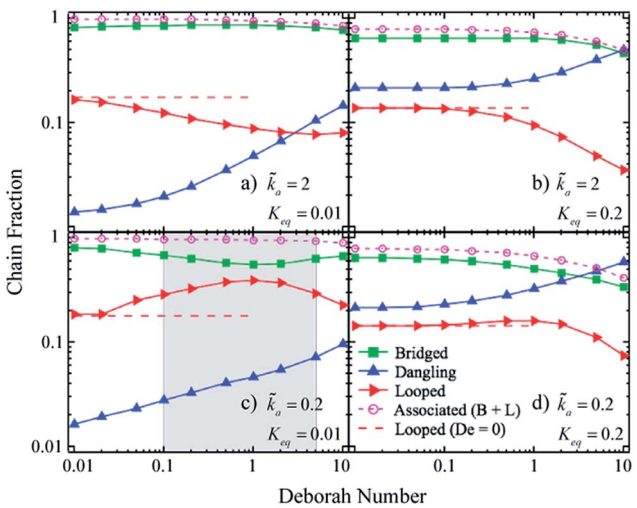

Fig. 4 Fractional chain distribution in steady shear flow for the four extreme cases studied in this work. K_{eq} increases along the horizontal axis and $\tilde{k}_a$ increases along the vertical axis. The lower left corner represents a system undergoing non-monotonic stress (shaded area). The corresponding non-monotonicities in chain fraction are a function of the balance between slow association kinetics and convection-assisted increases in extension.

Intuitively, the ratio of loops to dangling chains at steady state should decrease with increasing De, as the shear flow shifts the effective equilibrium between the two chain populations to favour dangling chains. This effect is clearly observed (Fig. S6†); however, the density of dangling chains increases sufficiently fast that the increased concentration results in an increase in the total number of loops (Fig. 4c). The increase in loops holds for De < 1, when chain ends are able to relax to near their equilibrium distribution despite convective forces.

It should be noted that the network is assumed to be homogeneous and percolating under all flow conditions. For this assumption to hold, it is necessary for the junction valency to be above the percolation threshold. This critical condition can be estimated using the Flory–Stockmayer equation such that the valency (z) of the chain ends must be greater than:[55]

$$z \geq \frac{1}{p} + 1. \quad (12)$$

Where p represents the fraction of bridged chains. Since the fraction of bridged chains is greater than 0.5 for most conditions explored, z must be larger than three to maintain a percolating network. Under some conditions, the fraction of bridged chains drops to 0.33, where z must be greater than 4 for the percolation assumption to hold.

This behaviour illustrates the importance of looped chains in the development of non-monotonic flow curves. By considering looped chains in the theory, the overall fraction of associated chains is higher than would be predicted in a model of bridged and dangling chains alone (Fig. 3). However, there are fewer elastically active chains when loops are included. When the same system with $K_{eq} = 0.01$ and $\tilde{k}_a = 0.2$ is solved with a zero probability of forming looped chains, the non-monotonicities present at steady state occur at higher values of both stress and shear rate (Fig. 4).

Effect of average chain extension on steady shear viscometric response

Because the shear stress in the gel derives directly from chain extension of bridged and dangling chains, understanding the average chain extension as a function of $\tilde{k}_a$, K_{eq}, and De is also critical to explaining the resulting stress curves. Without reaction terms, affinely deformed bridged chains will never reach a steady-state extension, while the extension of dangling chains is dependent upon the shear rate (Fig. S7a†). However, the

introduction of reaction terms introduces spatially-dependent chain conformation probability (Fig. S8†) and changes the steady-state behaviour of dangling and bridged chain extension (Fig. 5).

When $\tilde{k}_a$ is low (implying that k_d is also low at a given K_{eq}), bridges can extend for a significant period of time until they reach an extension where finite extensibility of the chains significantly accelerates dangling chain formation. At this point, the dangling chain is extended beyond its equilibrium value and it retracts. Because $\tilde{k}_a$ is lower than unity, this retraction process occurs until the steady-state extension is approached. Therefore, the equilibrium end-to-end separation is lower for dangling chains than bridged chains at low De and low $\tilde{k}_a$. Because $\tilde{k}_d$ is lower at lower K_{eq}, chains extend to a greater extent before breaking, leading to larger average extension in both bridged and dangling chains at low K_{eq} than at high K_{eq}.

In contrast, when $\tilde{k}_a$ is high, chains interconvert between bridged and dangling states with a rate much faster than the chain relaxation rate. Chains rapidly sample associated and dissociated states within a single relaxation time, causing both populations to display the same average chain extension. Thus, the bridged chain end-to-end distance decreases while the dangling chain end-to-end distance increases. The region of De below which bridged and dangling chains display the same extension narrows with decreasing K_{eq} as $\tilde{k}_d = K_{eq}/\tilde{k}_a$ decreases, slowing the rate of interconversion relative to the shear rate.

At high shear rates, the extension of dangling chains always exceeds that of bridged chains (blue lines in Fig. 5), an effect not captured in theories where the entire chain distribution is not modelled. In high De flows, chains are strongly extended such that force-activated chain detachment results in a higher effective value of K_{eq}, and the population of highly extended chains consists primarily of dangling chains. However, particularly at low K_{eq}, the chain population remains dominantly in the bridged state to minimize the energy of associating groups (Fig. 4a and c). This dominance of bridged chain conformation couples with lower bridged chain extension (Fig. 4 and 5). The

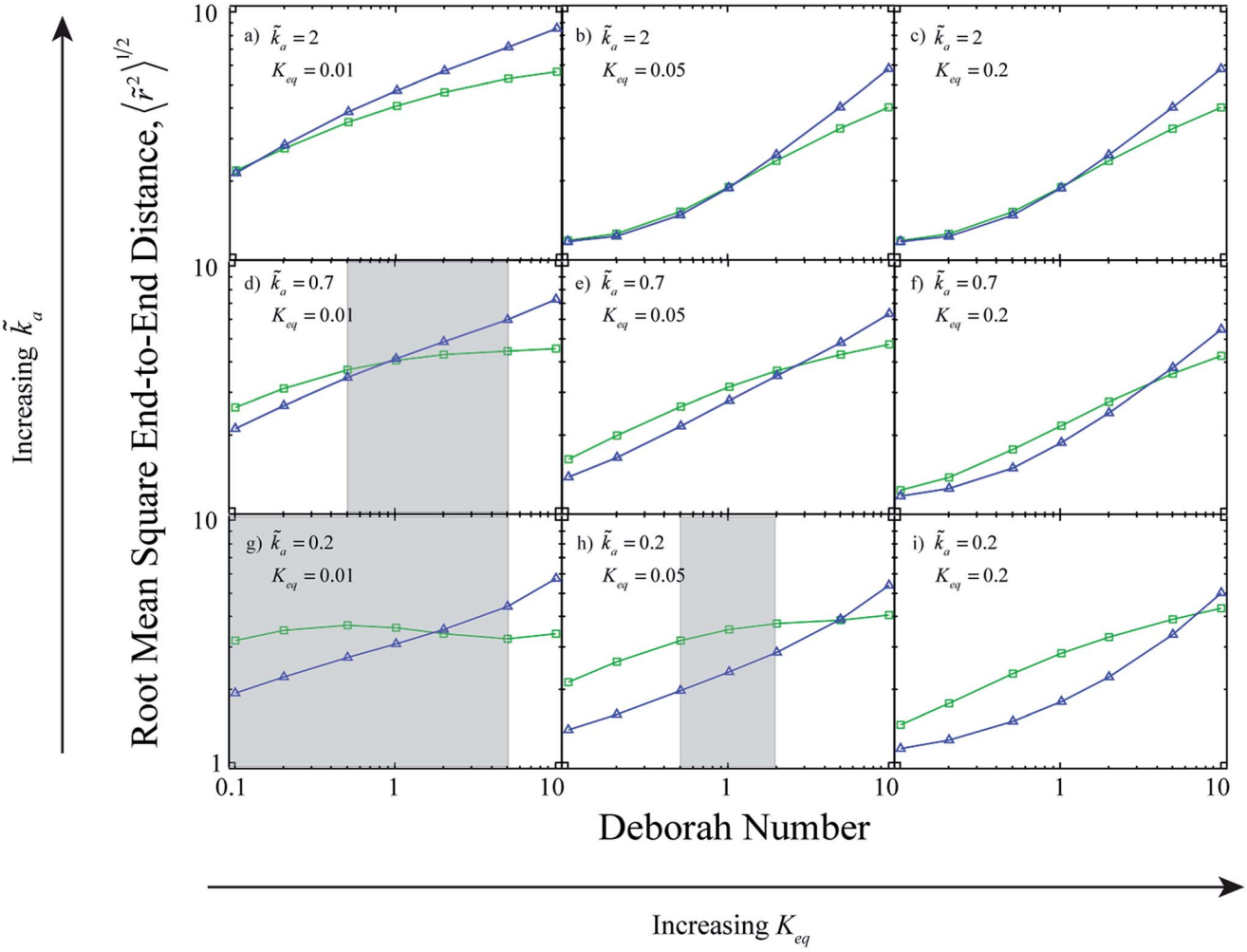

Fig. 5 Representative graphs of the root mean square end-to-end distance of a chain or non-monotonic (lower left) and monotonic (upper right) behaviour for various values of $\tilde{k}_a$ and K_{eq} (the equilibrium constant K_{eq} increases from left to right, the dimensionless rate constant $\tilde{k}_a$ increases from bottom to top). Shaded regions represent shear rates corresponding to non-monotonic steady state stress behaviour (d log $\tilde{\sigma}$/d log De < 0) as a function of De.

presence of a large bridged chain fraction with lower extension is due to chain tumbling. When chains become highly extended, they dominantly form dangling chains as illustrated in Fig. S8b.† However, these highly extended chains tend to align with the flow field, where lateral Brownian fluctuation of the chain end can result in sampling of the very low or negative velocity region of the local flow and lead to chain retraction (Fig. 6). This retraction results in an increased probability of bridge formation at lower chain extensions. The bridge then extends affinely with the network and a dangling end again reforms after the chain has re-extended. This tumbling mechanism can be verified by looking at the flux of the dangling chain ends.

$$\tilde{J} = \left[-(1/3)\tilde{\nabla}\psi - \psi \vec{F}_{\mathrm{FENE}} + \left(\mathrm{De}\cdot\tilde{r}_{\mathrm{y}}\psi\right)\right] \quad (13)$$

Eqn (13) is used in the calculation of the trajectories shown in Fig. 6. This behaviour is well known to occur on tethered DNA in shear flow.[56–58] The observation of such behaviour in this model is predicated upon the assumption of Rouse dynamics for the polymer chain model, such that rotational dynamics is not disrupted by interactions between polymers.

In all cases simulated, the extension of bridged chains slows or even reverses at higher De. The decrease in the rate of extension followed by a plateau can be explained by the bridge chain extensions approaching the finite extensibility limit, where the value of $\exp(\tilde{\beta}|\tilde{F}_{\mathrm{FENE}}|)$ exceeds 2 (see Fig. S5†) and bridged chains are rapidly destroyed by conversion into dangling chains. In the extreme case, this results in decreasing bridged chain extension for conditions corresponding to the lower left corner of Fig. 5. However, at higher shear rates, the extension again begins to increase as a result of tumbling dynamics of dangling chains promoting reformation of bridged chains. This occurs for all extensions.

Previous theories for associating polymer gels attribute the onset of non-monotonic flow curves in steady shear to the breaking of highly extended bridged chains to form less extended dangling chains, while each individual population increases in average extension monotonically with increasing De. However, this molecular picture does not take into account the potential role of chain tumbling. Chain tumbling results in the preservation of bridged chains to a higher shear rate than previously thought by enabling the formation of bridges from dangling chains that tumble and retract to a lower extension. This leads to a different origin of the non-monotonic stress in elastically active chains in this transient network theory not observed in previous theories. The calculations show that dangling chains are more extended than bridged chains at high De. While this effect dominates the onset of non-monotonicity at low flow rates (see Fig. 5, $\tilde{k}_{\mathrm{a}} = 0.2$, $K_{\mathrm{eq}} = 0.01$), chain tumbling at higher De leads to bridge chain extensions less than dangling chain extensions, creating a new tumbling contribution that effectively decreases average chain extension and can lead to unstable flows.

Start-up of steady shear flow

Much like in steady shear, the transient behaviour is a function of the balance between dangling and bridged chains as a function of location and relative shear rate. The behaviour seen for stress, extension, and chain fraction can again be explained by the molecular mechanisms responsible for the observed transient behaviour. When steady-state behaviour is monotonic, the transient behaviour exhibits a single stress overshoot at higher shear rates corresponding to the finite extensibility of bridged chains. In non-monotonic steady-state behaviour, dissociation events require force activation to occur on the timescale of flow and re-association events are less frequent. This results in dangling chains reaching a higher level of chain end extension at lower shear rates and results in chain end tumbling at lower shear rates than typically expected for non-

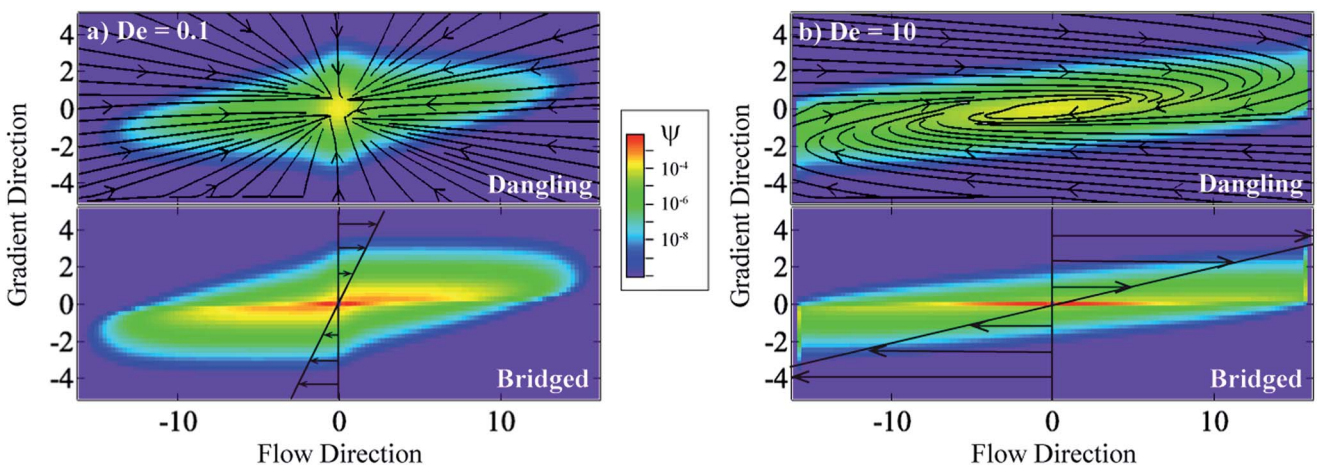

Fig. 6 Slices of three-dimensional probability distributions of dangling and bridged chains for a system with $\tilde{k}_{\mathrm{a}} = 0.2$ and $K_{\mathrm{eq}} = 0.01$ for (a) De = 0.1 and (b) De = 10 taken at the midplane of the vorticity direction. Streamlines in the plots of dangling chain distributions show the direction of dangling chain flux at the respective shear rate. Arrows denoting the imposed rheologic flow profile are illustrated on the bridged chain distribution and for clarity are not to scale.

reactive dangling chain ends. The tumbling of these dangling chain ends leads to multiple relaxation timescales correlating with the interchange between dangling and bridged chain ends as a function of their extension and decreases the total fraction of elastically effective chains by enabling the increase in looped chain fraction.

Analysis of transient data further illustrates the role of finite extensibility, chain end tumbling, interconversion rate, and conformation in the rheological response of transient networks. When interconversion events are not permitted, dangling chains asymptotically approach a limiting plateau in their elongation as a function of the applied shear rate, and bridged chains deform affinely with the network (Fig. S7a†). The corresponding stress during start-up of steady shear in bridged chains increases linearly with a slope of $(\partial \ln \tilde{\sigma}/\partial \ln(\tilde{t}\mathrm{De})$ where $\tilde{t}De = (\dot{\gamma}\tau)(t/\tau) = \dot{\gamma}t =$ strain) corresponding to the spring constant of the polymer chain where $\tilde{t}$De corresponds to the strain, and dangling chains approach a plateau value at which spring retraction and drag forces balance (Fig. S7b†).

While the presence of non-monotonicity in start-up of steady shear does not predict the presence of non-monotonicities in steady state flow,[59] the transient behaviour under conditions where non-monotonic flow profiles are observed exhibits multiple relaxation times. At high $\tilde{k}_a$ and K_{eq}, the total stress in the system (Fig. 7d) at low strain increases with a slope of one corresponding to the force of chain retraction in the limit where the spring force can be approximated as a Hookean spring (Fig. S7b†). As the applied strain increases, a stress overshoot is observed, followed by a plateau steady-state stress. This stress plateau is higher than that observed in the dangling chains alone as a result of the fast interchange between dangling and bridged chains such that dangling chains are stretched beyond their equilibrium extension (Fig. 7b and S9a†). As the imposed shear rate is increased, the stress plateau is preceded by an increasingly large stress overshoot caused by chain finite extensibility. Non-reactive dangling chains can also exhibit minor stress overshoots at high shear as evidenced in Fig. S7b.† These overshoots are qualitatively similar to those seen by Shull *et al.* on triblock copolymers of poly(methyl methacrylate) and poly(*n*-butyl acrylate).[31] Shull's experimental results showed an overshoot of approximately 11.75 dimensionless stress units – or a single order of magnitude difference – at De = 2.4. The overshoot for De = 2 in Fig. 7a is just under a single order of magnitude while the overshoot for De = 5 is just over an order of magnitude. This overshoot occurs in tandem with decreases in the fractions of bridged and looped chains and increases in the fractions of dangling chains (Fig. 7c).

The transient behaviour corresponding to a non-monotonic steady flow curve exhibits multiple relaxation events at higher shear rates. Much like in the monotonic case, the slope of the transient stress growth at low strain corresponds to the elastic contribution of the system. However, the initial stress

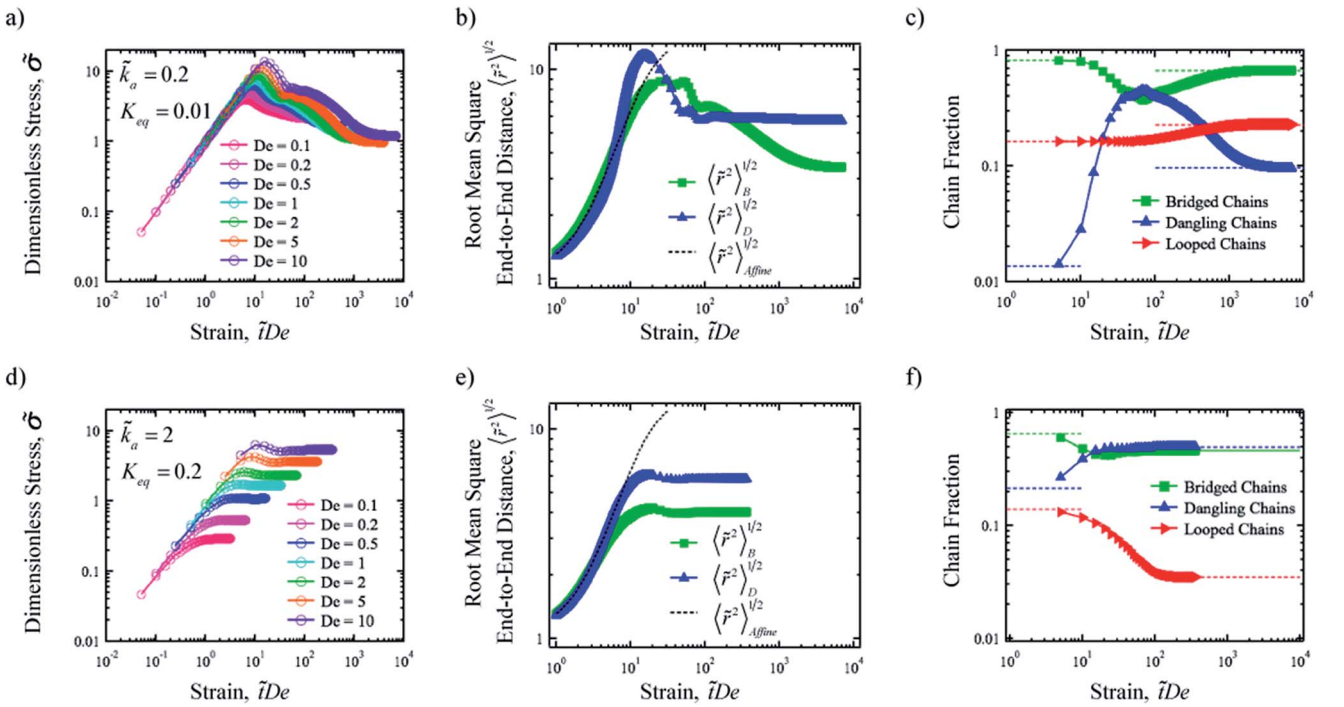

Fig. 7 Start-up of steady shear for a system corresponding to a monotonic (d–f) and a non-monotonic (a–c) steady flow curve demonstrating the development of multiple relaxation events for systems exhibiting non-monotonic flow curves at steady state. Parts (a) and (d) represent stress for all De at the specified values of $\tilde{k}_a$ and K_{eq} while the remaining figures represent chain extension and fraction for De = 10. For the monotonic case, stress overshoots are the result of chain finite extensibility. For the non-monotonic case, stress overshoots correspond to a combination of chain tumbling, finite chain extensibility, and the conversion between dangling and looped chains resulting in decreased extension of the bridged chains. The dashed lines in (c) and (f) represent equilibrium and steady-state chain fractions at time $\tilde{t} = 0$ and $\tilde{t} = \infty$, respectively. The dashed lines in (b) and (e) represent the extension of a chain undergoing affine network deformation.

overshoots present at all shear rates correspond to a combination of chain finite extensibility and dangling chain tumbling (De > 1) or chain relaxation (De ≤ 1). At the lower equilibrium values corresponding to non-monotonic steady flow curves, bridged chain dissociation on the timescale of flow requires force activation such that bridged chains reach high levels of extension prior to dissociation, even at low shear rates.

The relaxations following the initial chain extension overshoot/stress overshoot in Fig. 7a for De = 10 result from oscillations between dangling and bridged chains during tumbling. When the dangling chains retract during tumbling, they reach a level of extension at which bridged chains can again be formed (corresponding to the crossover in Fig. 7b). The bridged chains then stretch again until they undergo force-activated detachment from the network to become dangling chains that again tumble. This cyclical stretching and extension yields a ringing timescale in the stress response in start-up shear. While the response is initially large because the initial shear results in a rapid transition of a population of bridges to dangling chains over a short period of time, de-phasing of the chain state over several tumbling cycles damps the oscillation in stress to give a steady state plateau at long times where $\tilde{t}$De > 1000 (Fig. 7a). The looped chain fraction begins to increase during the initial system-wide tumbling of dangling chains. This is possible because the tumbling chain ends are swept back toward the region where looped chain formation is again favoured (Fig. S8a†).

Stress relaxation following shear

The stress relaxation of dangling chains following cessation of steady shear follows a single exponential decay resulting from dangling chain relaxation. Upon incorporation of reaction terms, the total stress of the system relaxes *via* a series of exponential decays, indicating the presence of more than a single relaxation process. Because bridged chains do not deform under quiescent conditions, the relaxation rate becomes a function of the dangling chain relaxation and the fraction of chains able to relax as associated chains interconvert with dangling chains. Evidence of these multiple relaxation phenomena can be seen in graphs of the transient evolution in the stress, chain fraction, and extension (Fig. 8). When the kinetics of association are fast and $1/\tilde{k}_a < 1$, the rate of chain inter-conversion occurs faster than the rate of chain relaxation. This inter-conversion results in a single relaxation event on the order of $\tilde{t}_{heal} \propto \tilde{t}\psi_D$ as chains dynamically attach and detach from the network multiple times in order to fully relax, hindering the relaxation rate by a factor approximately equal to the fraction of dangling chains.

For systems with low $\tilde{k}_a$ values ($1/\tilde{k}_a < 1$), a series of two discrete relaxation events occurs because dangling chains are able to fully relax before they reattach to the network. The first relaxation corresponds to the relaxation of the dangling chains present after cessation of shear. This initial relaxation time occurs on times $\tilde{t} \sim O(\tau)$. The second relaxation event involves

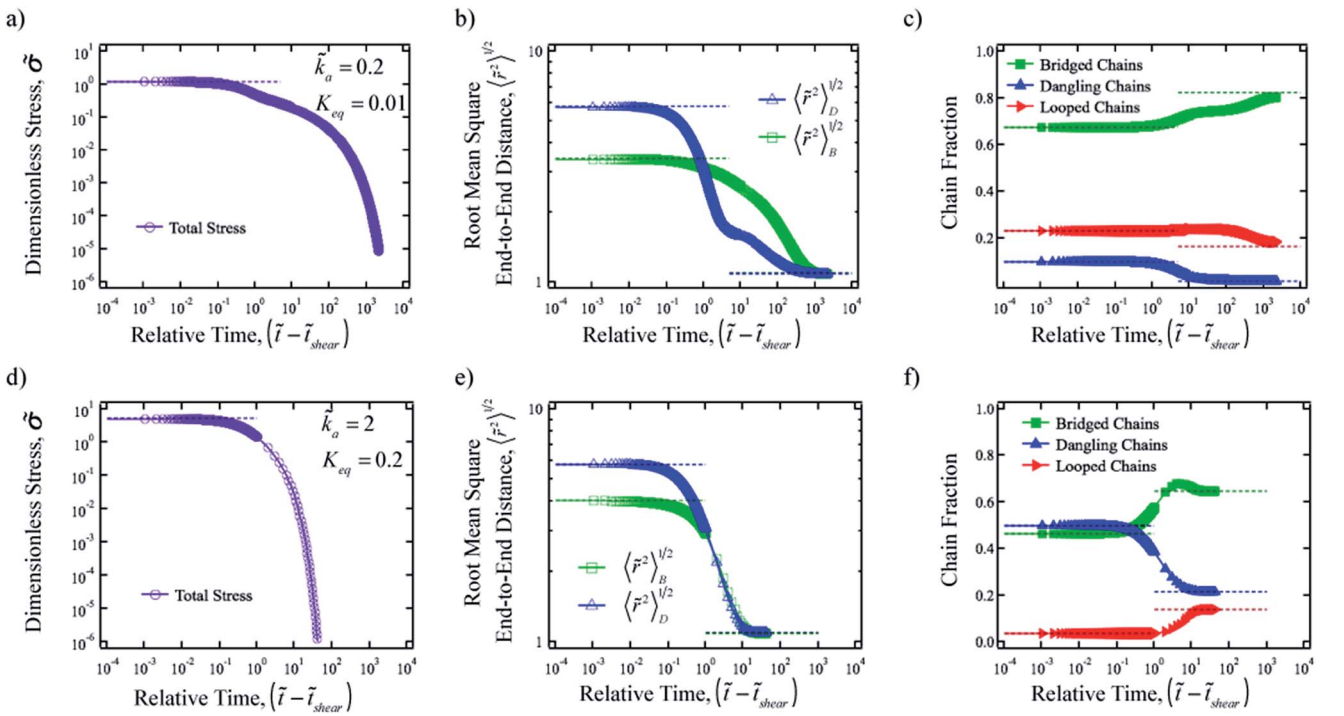

Fig. 8 Stress relaxation data for the two system extremes addressed in this work where (a)–(c) corresponds to $\tilde{k}_a = 0.2$, $K_{eq} = 0.01$ and (d)–(f) corresponds to $\tilde{k}_a = 2$, $K_{eq} = 0.2$ following a shear rate of De = 10. The relative time in all plots represents the elapsed time following cessation of steady-state shear at $\tilde{t}_{shear}$, the time to reach steady-state in start-up shear flow. In the units of dimensionless time, the relaxation time for a non-associating polymer chain is 1. For all plots, dashed lines represent steady-state shear and stagnant conditions. When $1/\tilde{k}_a > 1$ (a–c), dangling chains are able to relax on time scales the order of τ (*i.e.* $\tilde{t} - \tilde{t}_{shear} \leq 1$) prior to undergoing a second, association/dissociation rate-dependent relaxation process. This additional time scale contributes to the longer relaxation time required for the system in (a)–(c) to relax relative to the system in (d)–(f).

the dissociation-dependent relaxation of the rest of the system. Since dangling chains are the only portion of the system capable of relaxing, the dissociation kinetics determine the fraction of chains that have detached from the network and had an opportunity to relax. Following high shear rates, this recovery becomes a function first of the exchange between dangling and bridged chains and then of the exchange between all three conformations as a function of dangling chain extension.

Start-up of steady shear and steady shear flow are heavily dependent upon both kinetics and shear-induced phenomena such as chain tumbling and force-activated dissociation following Bell's Law (eqn (3)). While chain tumbling does not occur in low shear, stress relaxation remains a function of both kinetics and the degree of chain extension because the bridge dissociation rate is strongly modulated by the degree of extension. Therefore, relaxation processes can become more broadly spread in time due to the fact that highly extended chains will relax rapidly but less extended chains will relax slowly.

At high shear rates, the time scales corresponding to kinetic interchange become a strong function of chain extension. Specifically, dangling chains cannot associate to become looped chains until their extension is low enough to promote looped chain formation, approximately below $\tilde{r} = 2$. The system is incapable of fully relaxing to equilibrium until dangling, bridged, and looped chains have the ability to equilibrate. This is evidenced in Fig. 8c, where the bridged chain fraction begins to increase following the initial dangling chain association. Once the chain extension of dangling chains reaches a distance where the probability of forming looped chains is non-zero (Fig. S8†), the fraction of looped chains also increases. Increasing the time between association and dissociation events not only results in steady shear non-monotonicities and increased yield stresses but also increased recovery times post-shear despite lower steady-state stress values. Recent work[14] has shown a correlation between larger end-block lengths (corresponding to slower chain end association/dissociation kinetics) and increased relaxation times.

Indei and Takimoto recently looked at multi-sticker polymers in oscillatory shear flow. The characteristics detailed here which result in longer relaxation times also contribute in oscillatory shear flow.[60] When multiple stickers are used (*i.e.* – non-telechelic systems), Indei and Takimoto show evidence of associative Rouse behaviour. The chain behaviour becomes dependent not only upon the relaxation behaviour of each individual association but also on the total network relaxation behaviour.[60] Semenov *et al.* experimentally and theoretically show similar behaviour for hyaluronan-based associating polymers.[26] This suggests that when the system here is translated to a chain with multiple stickers, internal relaxations will further retard the system dynamics. However, the overall picture of the relative kinetics and sticker locations determining the dynamics should remain largely unchanged.

Conclusions

A new formulation of transient network theory was developed based on reaction-diffusion Smoluchowski equations for loops, bridges, and dangling chains in a telechelic polymer gel. Numerical solution of the model yields time-dependent end-to-end distributions for chains that reveal the importance of both looped chains and chain tumbling on the mechanical response of these networks. The importance of end group sticker kinetics on telechelic network behaviour was explored in detail, providing insight into the molecular behaviour responsible for non-monotonic flow curves. By adjusting the kinetic rates of sticker association and dissociation and respective kinetic equilibrium, it is possible to control shape and monotonicity of the flow curve. We have shown that non-monotonic flow profiles only occur at low values of $\tilde{k}_a$ and K_{eq}, with both loop formation and extension of elastically active chains playing an important role.

In systems with non-monotonic flow curves, loop formation first increases, then decreases with increasing De. Non-monotonicities also occur in the stress per elastically effective chain, indicating that they are observed in the absence of loops due to decreased chain extension. However, the inclusion of looped chains in the model causes the non-monotonicities to appear at lower De and lower stress. Chain tumbling is also observed in this model for a physically associated gel, corresponding to the observation of non-monotonic Deborah number verses chain extension curves in bridged chains and enabling a large fraction of chains to remain in the associated state even at high De.

The interchanges between bridged and dangling chain ends during start-up of steady shear flow result in multiple chain relaxation events. An initial stress overshoot results when bridged chains undergo force-activated conversion to dangling chains, and in gels that show non-monotonic stress profiles, the chain tumbling leads to damped oscillations that decay as the chain population equilibrates towards the final steady flow. Similarly, during stress relaxation when the fraction and availability of dangling chains is crucial, the relaxation time depends on the relative kinetic rates. When the kinetics of interchange occur on time scales equivalent to or faster than chain relaxation ($1/\tilde{k}_a < 1$), the total system relaxation time is on the order of τ. However, decreasing the rates of association and dissociation results in a total relaxation time significantly greater than τ which is primarily dominated by the value of $1/\tilde{k}_d$. This new transient network theory shows that both looped chains and chain tumbling are potentially important effects in associating polymer networks, providing new insight into the rheology of physical gels and our fundamental understanding of one of the most pervasive categories of soft materials.

Acknowledgements

This research was supported by the U. S. Army Research Office through the Institute of Soldier Nanotechnologies. M.K.S. was supported by the Department of Defense (DoD) through the National Defense Science and Engineering Graduate Fellowship (NDSEG) Program.

Notes and references

1 A. Richter, G. Paschew, S. Klatt, J. Lienig, K. F. Arndt and H. J. P. Adler, *Sensors*, 2008, **8**, 561–581.

2 S. Nayak and L. A. Lyon, *Angew. Chem., Int. Ed.*, 2005, **44**, 7686–7708.
3 C. Wang, N. T. Flynn and R. Langer, *Adv. Mater.*, 2004, **16**, 1074–1079.
4 C. Y. Hou, Q. H. Zhang, Y. G. Li and H. Z. Wang, *J. Hazard. Mater.*, 2012, **205**, 229–235.
5 M. M. Nasef and O. Guven, *Prog. Polym. Sci.*, 2012, **37**, 1597–1656.
6 C. Q. Yan and D. J. Pochan, *Chem. Soc. Rev.*, 2010, **39**, 3528–3540.
7 H. Bae, H. H. Chu, F. Edalat, J. M. Cha, S. Sant, A. Kashyap, A. F. Ahari, C. H. Kwon, J. W. Nichol, S. Manoucheri, B. Zamanian, Y. D. Wang and A. Khademhosseini, *J. Tissue Eng. Regener. Med.*, 2014, **8**, 1–14.
8 X. H. Zhao, *Soft Matter*, 2014, **10**, 672–687.
9 M. J. Glassman, J. Chan and B. D. Olsen, *Adv. Funct. Mater.*, 2012, **23**(9), 1182–1193.
10 R. A. Cone, *Adv. Drug Delivery Rev.*, 2009, **61**, 75–85.
11 B. Ozbas, J. Kretsinger, K. Rajagopal, J. P. Schneider and D. J. Pochan, *Macromolecules*, 2004, **37**, 7331–7337.
12 R. V. Rughani, M. C. Branco, D. Pochan and J. P. Schneider, *Macromolecules*, 2010, **43**, 7924–7930.
13 N. Holten-Andersen, M. J. Harrington, H. Birkedal, B. P. Lee, P. B. Messersmith, K. Y. C. Lee and J. H. Waite, *Proc. Natl. Acad. Sci. U. S. A.*, 2011, **108**, 2651–2655.
14 M. J. Glassman and B. D. Olsen, *Soft Matter*, 2013, **9**, 6814–6823.
15 M. Guvendiren, H. D. Lu and J. A. Burdick, *Soft Matter*, 2012, **8**, 260–272.
16 K. Kataoka, A. Harada and Y. Nagasaki, *Adv. Drug Delivery Rev.*, 2001, **47**, 113–131.
17 R. Duncan, *Nat. Rev. Drug Discovery*, 2003, **2**, 347–360.
18 R. Langer and D. A. Tirrell, *Nature*, 2004, **428**, 487–492.
19 K. Y. Lee and D. J. Mooney, *Chem. Rev.*, 2001, **101**, 1869–1879.
20 M. Rubinstein and R. H. Colby, *Polymer Physics*, Oxford University Press, New York, 2003.
21 P. J. Flory, *Principles of Polymer Chemistry*, Cornell University Press, Ithaca, NY, 1953.
22 M. S. Green and A. V. Tobolsky, *J. Chem. Phys.*, 1946, **14**, 80–92.
23 F. Tanaka and S. F. Edwards, *Macromolecules*, 1992, **25**, 1516–1523.
24 T. Annable, R. Buscall, R. Ettelaie and D. Whittlestone, *J. Rheol.*, 1993, **37**, 695–726.
25 A. N. Semenov, J. F. Joanny and A. R. Khokhlov, *Macromolecules*, 1995, **28**, 1066–1075.
26 A. Semenov, A. Charlot, R. Auzely-Velty and M. Rinaudo, *Rheol. Acta*, 2007, **46**, 541–568.
27 A. N. Semenov and M. Rubinstein, *Macromolecules*, 1998, **31**, 1373–1385.
28 J. G. H. Cifre, T. M. A. O. M. Barenbrug, J. D. Schieber and B. H. A. A. van den Brule, *J. Non-Newtonian Fluid Mech.*, 2003, **113**, 73–96.
29 B. H. A. A. Vandenbrule and P. J. Hoogerbrugge, *J. Non-Newtonian Fluid Mech.*, 1995, **60**, 303–334.
30 W. C. Yount, D. M. Loveless and S. L. Craig, *Angew. Chem., Int. Ed.*, 2005, **44**, 2746–2748.
31 K. A. Erk and K. R. Shull, *Macromolecules*, 2011, **44**, 932–939.
32 M. E. Seitz, W. R. Burghardt, K. T. Faber and K. R. Shull, *Macromolecules*, 2007, **40**, 1218–1226.
33 K. C. Tam, R. D. Jenkins, M. A. Winnik and D. R. Bassett, *Macromolecules*, 1998, **31**, 4149–4159.
34 E. Michel, J. Appell, F. Molino, J. Kieffer and G. Porte, *J. Rheol.*, 2001, **45**, 1465–1477.
35 A. Tripathi, K. C. Tam and G. H. McKinley, *Macromolecules*, 2006, **39**, 1981–1999.
36 R. S. Hoy and G. H. Fredrickson, *J. Chem. Phys.*, 2009, **131**, 224902.
37 C. E. Sing and A. Alexander-Katz, *Macromolecules*, 2012, **45**, 6704–6718.
38 M. Wilson, A. Rabinovitch and A. R. C. Baljon, *Phys. Rev. E: Stat., Nonlinear, Soft Matter Phys.*, 2011, **84**, 061801.
39 S. Tallury, R. Spontak and M. Pasquinelli, *Polym. Prepr.*, 2012, **53**, 47.
40 C. E. Sing and A. Alexander-Katz, *Macromolecules*, 2011, **44**, 6962–6971.
41 R. G. Larson, *The Structure and Rheology of Complex Fluids*, Oxford University Press, New York, 1999.
42 R. B. Bird, C. F. Curtiss, R. C. Armstrong and O. Hassager, *Dynamics of Polymeric Liquids*, John Wiley & Sons, Inc, 1987, vol. II.
43 M. Doi and S. F. Edwards, *The Theory of Polymer Dynamics*, Oxford University Press, Inc., New York, NY, 2001.
44 G. I. Bell, *Science*, 1978, **200**, 618–627.
45 D. E. Makarov, *J. Chem. Phys.*, 2011, **135**, 194112.
46 P. Hanggi, P. Talkner and M. Borkovec, *Rev. Mod. Phys.*, 1990, **62**, 251–341.
47 I. W. Hamley, S. D. Connell and S. Collins, *Macromolecules*, 2004, **37**, 5337–5351.
48 M. Guvendiren, D. L. Hoang and J. A. Burdick, *Soft Matter*, 2012, **8**, 260–272.
49 M. Kim, S. C. Tang and B. D. Olsen, *J. Polym. Sci., Part B: Polym. Phys.*, 2013, **51**, 587–601.
50 I. W. Hamley, *Block Copolymers in Solution: Fundamentals and Applications*, John Wiley & Sons Inc., 2005.
51 G. Recktenwald, *Numerical Methods with Matlab: Implementation and Application*, Prentice Hall, Upper Saddle River, NJ, 2000.
52 P. D. Olmsted, *Rheol. Acta*, 2008, **47**, 283–300.
53 Y. Kwon, *J. Non-Newtonian Fluid Mech.*, 1999, **88**, 89–98.
54 R. L. Moorcroft and S. M. Fielding, *Phys. Rev. Lett.*, 2013, **110**, 086001.
55 P. J. Flory, *J. Am. Chem. Soc.*, 1941, **63**, 3083–3090.
56 R. Delgado-Buscalioni, *Phys. Rev. Lett.*, 2006, **96**, 088303.
57 P. S. Doyle, B. Ladoux and J. L. Viovy, *Phys. Rev. Lett.*, 2000, **84**, 4769–4772.
58 C. A. Lueth and E. S. G. Shaqfeh, *Macromolecules*, 2009, **42**, 9170–9182.
59 R. L. Moorcroft and S. M. Fielding, *J. Rheol.*, 2014, **58**, 103–147.
60 T. Indei and J. Takimoto, *J. Chem. Phys.*, 2010, **133**, 194902.

